

The Effect of Instrumentation on Sports Balls During Flight, Exemplified by A Smart AFL Ball: Model and Experiment [†]

Franz Konstantin Fuss

Smart Products Engineering[†] Program, Centre for Design Innovation, Swinburne University of Technology, Melbourne, VIC 3122, Australia; fkfuss@swin.edu.au; Tel.: +61-3-9214-6882

[†] Presented at the 13th conference of the International Sports Engineering Association, Online, 22–26 June 2020.

Published: 15 June 2020

Abstract: Sensors incorporated in a sports ball for data collection can affect the properties of a ball, specifically the spin rate of a ball if the mass distribution (moments of inertia, MOI) is altered. This paper provides a method for assessing the MOIs of a smart ball by means of spin rate data, collected from a gyroscopic sensor. The critical elevation angle of the angular velocity vector defines the separatrix condition, which decides whether the angular velocity vector precesses about the axis with the greatest MOI or with the smallest MOI. The critical elevation angle can be directly determined from the experimental of the angular velocity data, and, together with the ratio of precession speed to angular velocity, applied to calculating the three MOIs. In the smart AFL ball used for the experiments, the critical angle was 13.5°, and the ratio of the two small MOIs was 1.014.

Keywords: instrumentation; gyroscope; spin axis; smart balls; Australian football; moment of inertia; polhodes; separatrix condition; critical angular velocity vector angle

1. Introduction

Smart balls are becoming more popular with the technical improvements of lightweight batteries, miniaturised electronics and long-range wireless data transfer. In addition to electronics considerations, putting instrumentation into a ball can affect the dynamics of the ball:

- The mass of sports balls is regulated and must not be affected by electronic items;
- The mass concentration, i.e., the centre of mass (COM), must remain in its original location, as the ball rotates about the COM during flight, and any COM offset can influence the ball's aerodynamics;
- The mass distribution, i.e., the moments of inertia (MOI) should not be changed too much, as the MOI affects the rotational behaviour of the ball (spin rate).

It is therefore obvious that any instrumentation of a ball has to be designed carefully and tested extensively. The influence of a changed MOI can be assessed easily if the ball is instrumented with a gyroscopic sensor (gyro). If the spin axis moves (i.e., precesses) with respect to the body coordinate system (BCS, i.e., the ball's, or more precisely, the gyro sensor's coordinate system), then either the ball wobbles or the instrumentation has an effect on the MOI. Furthermore, the three MOIs of spherical sports balls are not necessarily identical even without instrumentation. Seams, valves, laces, and material distribution affect the MOIs.

The aim of this paper is to “reverse-engineer” the conditions of a ball's MOIs from gyro data.

2. Model

The three MOIs about the axes of the BCS are denoted I_1 , I_2 , and I_3 . The instantaneous angular velocity vector (spin axis) is denoted ω_1 , ω_2 , and ω_3 . The intersection lines of the moving (precessing) ω -vector and the ball's surface are defined by the intersection of two ellipsoids, based on the conservation of two physical properties [1]:

- Conservation of angular momentum, H , defines the angular momentum ellipsoid:

$$H^2 = (I_1\omega_1)^2 + (I_2\omega_2)^2 + (I_3\omega_3)^2 = const . \tag{1}$$

- Conservation of rotational kinetic energy, T , defines the kinetic energy ellipsoid:

$$2T = I_1\omega_1^2 + I_2\omega_2^2 + I_3\omega_3^2 = const . \tag{2}$$

The position of the unit ω -vector has to satisfy two conditions, derived from re-arranging Equations (1) and (2):

$$\frac{\omega_1^2}{(H/I_1)^2} + \frac{\omega_2^2}{(H/I_2)^2} + \frac{\omega_3^2}{(H/I_3)^2} = 1 \tag{3}$$

and

$$\frac{\omega_1^2}{2T/I_1} + \frac{\omega_2^2}{2T/I_2} + \frac{\omega_3^2}{2T/I_3} = 1. \tag{4}$$

It follows from Equations (3) and (4) that

$$\frac{2T}{I_{1,2,3}} = \left(\frac{H}{I_{1,2,3}} \right)^2. \tag{5}$$

The two ellipsoids (H - and T -) intersect, and the curve of intersection, the so-called polhode, is the path of the angular velocity vector with respect to the BCS. In prolate spheroids (oval balls, such as for rugby, Australian rules football and American football), the ω -vector can rotate about the long (major) axis or about the short (minor) one. Figure 1 exemplifies this behaviour.

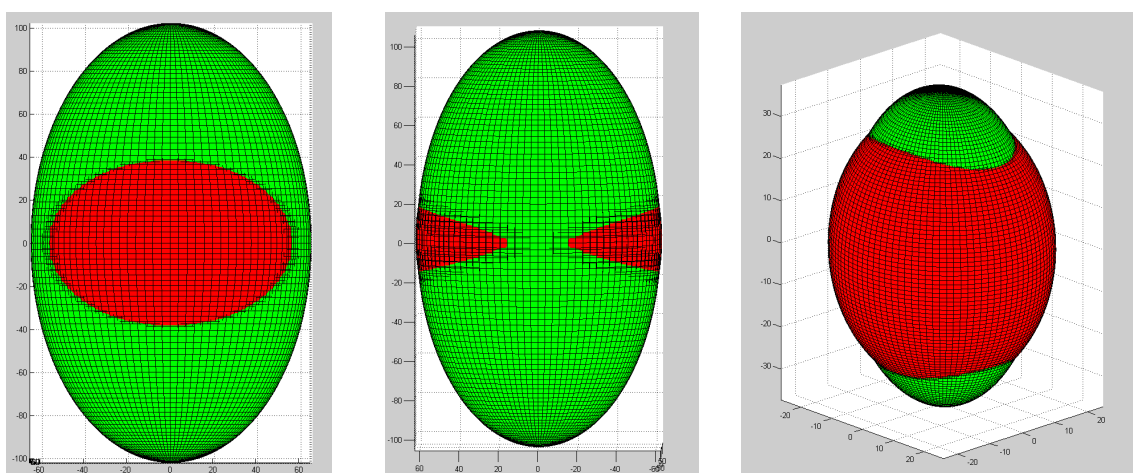


Figure 1. Angular momentum and kinetic energy ellipsoids of a prolate spheroid. The two left subfigures show the polhode (intersection of the two ellipsoids) about a minor axis of the prolate spheroid, in front view and side view. Note that there are two solutions and the ω -vector follows either the front or back polhode. If the two solutions merge, then the ω -vector follows either the top or bottom polhode (counterclockwise or clockwise spin) shown in the right subfigure.

Subtracting Equation (3) from Equation (4) and multiplying the result by H^2 yields the polhode equation

$$\omega_1^2 I_1 \left(I_1 - \frac{H^2}{2T} \right) + \omega_2^2 I_2 \left(I_2 - \frac{H^2}{2T} \right) + \omega_3^2 I_3 \left(I_3 - \frac{H^2}{2T} \right) = 0. \tag{6}$$

For real solutions of Equation (6), the three coefficients cannot have the same sign, and

$$I^* = \frac{H^2}{2T} \tag{7}$$

where I^* is defined as follows: if $I_1 > I_2 > I_3$, then $I_1 \geq I^* \geq I_3$.

Projecting the polhode equation, i.e., Equation (6), on the ω_1 - ω_3 plane yields

$$\omega_1^2 I_1 (I_1 - I_2) + \omega_3^2 I_3 (I_3 - I_2) = 2T(I^* - I_2). \tag{8}$$

If $I^* = I_2$, then we obtain the separatrix condition

$$\omega_1^2 I_1 (I_1 - I^*) + \omega_3^2 I_3 (I_3 - I^*) = 0, \tag{9}$$

namely, the decision condition that determines whether the ω -vector rotates about the axis with the greatest MOI (I_1) or about the axis with the smallest MOI (I_3). This principle excludes a stable rotation about the axis with the intermediate MOI (I_2)

Equation (9) delivers the critical angle of the ω -vector, namely θ_{crit} , from

$$\frac{\omega_3^2}{\omega_1^2} = \tan^2 \theta_{crit} = -\frac{I_1(I_1 - I^*)}{I_3(I_3 - I^*)} = -\frac{I_1(I_1 - I_2)}{I_3(I_3 - I_2)} \tag{10}$$

and

$$\theta_{crit} = \tan^{-1} \sqrt{-\frac{I_1(I_1 - I_2)}{I_3(I_3 - I_2)}}. \tag{11}$$

If the pitch angle of the ω -vector with respect to the ω_1 - ω_2 plane is smaller or greater than θ_{crit} , then the spin axis precesses about the minor (with the greatest MOI I_1) or major ball axis (with the smallest MOI I_3), respectively.

According to Fuss and Smith [2],

$$\frac{\Omega}{\omega_R} = \left(\frac{I_3 - I_{1,2}}{I_{1,2}} \right) \cos \left(\frac{\pi}{2} - \theta_{crit} \right), \tag{12}$$

where ω_R and Ω are the resultant angular velocity, i.e., $\sqrt{(\omega_1^2 + \omega_2^2 + \omega_3^2)}$, and the precession rate, respectively. The precession rate is the speed at which the ω -vector moves about the minor or major axes. From Equation (12), when plotting Ω/ω_R against $\cos(\pi/2 - \theta_{crit})$, the gradient of the regression fit corresponds to $(I_3 - I_{1,2})/I_{1,2}$ [2]. Ω/ω_R and $\cos(\pi/2 - \theta_{crit})$ are determined experimentally from a ball instrumented with a gyro.

Solving Equation (11) for I_2 yields

$$I_2 = \frac{I_1^2 + I_3^2 (\tan^2 \theta_{crit})}{I_1 + I_3 (\tan^2 \theta_{crit})}. \tag{13}$$

If I_1 and I_3 are known, or at least the ratio I_1/I_3 or I_3/I_1 , then I_2 can be determined directly, or relative to I_1 . If $\theta_{crit} = 0^\circ$ (ω -vector in ω_1 - ω_2 plane), then Equation (13) reduces to $I_2 = I_1$. If $\theta_{crit} = 90^\circ$ (ω -vector perpendicular to the ω_1 - ω_2 plane) then $\tan^2\theta_{crit} = \infty$, and Equation (13) reduces to $I_2 = I_3$.

3. Experiment

The experiments were carried out with the smart AFL ball developed by, and described in, Fuss and Smith [2] and Fuss et al. [3]. The angular velocity ω and its three components (ω_1 , ω_2 , and ω_3 .) with respect to the BCS were measured with a gyro. The data from these two references were analysed further. The precessing ω -vectors were reconstructed in 3D in AutoCAD 2000 (Autodesk, San Rafael, CA, USA) with respect to the ball, as well as plotted on an elevation (pitch) vs. azimuth (yaw) diagram (where the yaw angle is the position of the ω -vector projected onto the ω_1 - ω_2 plane, and the pitch angle θ is the included angle between ω -vector and ω_1 - ω_2 plane). The task was to find ω -vectors, precessing very close to, and on either side of, the separatrix condition, in order to determine θ_{crit} . From Equation (13), I_2 was estimated and compared to I_1 .

4. Results

Figure 2 shows ω -vectors at different θ -angles, precessing about the major axis of the ball (Figure 2a–c) and the minor axis (Figure 2d).

Figure 3 explains how θ_{crit} was determined, which was approximately 13.5° . From Fuss and Smith [2], by applying Equation (12), $(I_3 - I_{1,2})/I_{1,2}$ was 0.42, resulting in $I_{1,2}/I_3$ of 1.724. When normalizing the MOIs to I_3 , then $I_3 = 1$, and $I_{1,2} = 1.724$. Yet, if $\theta_{crit} > 0^\circ$, then $I_1 \neq I_2$. Finding I_2 from Equation (13), considering that $I_{1,2} = (I_1 + I_2)/2$, delivers the following results: $I_1 = 1.736$, $I_2 = 1.712$, and $I_1/I_2 = 1.014$. The latter ratio teaches that I_1 is only 1.4% greater than I_2 .

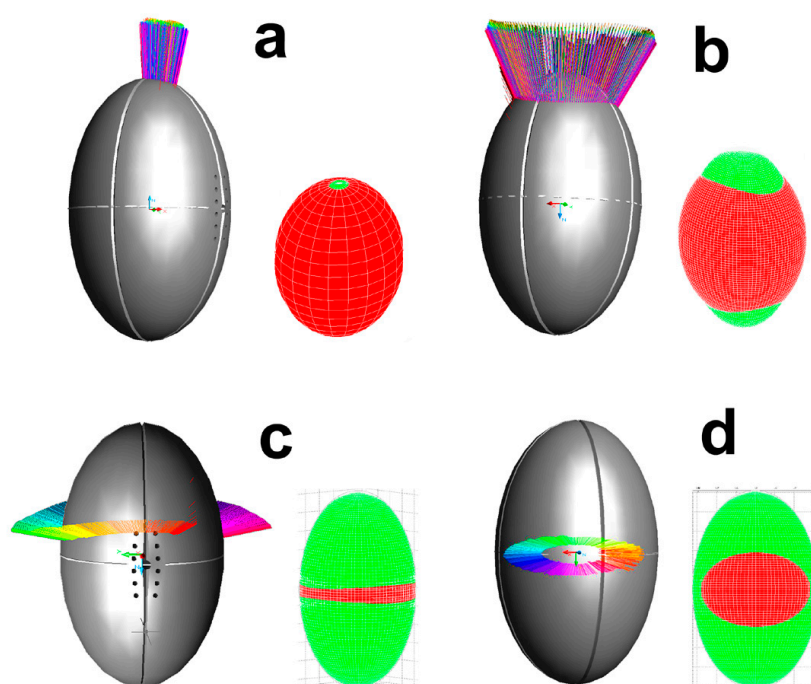


Figure 2. ω -vectors (colour-coded) projected on the surface of an AFL ball and the corresponding ellipsoids: (a) almost-perfect torpedo punt, the ball spins about the major axis of the ball and ω precesses about the major axis; (b) imperfect torpedo punt, the ball spins about the major axis and ω precesses about the major axis; (c) imperfect drop punt, the ball spins about the minor axis of the ball and ω precesses about the major axis; (d) almost-perfect drop punt, the ball spins about the minor axis of the ball and ω precesses about the minor axis.

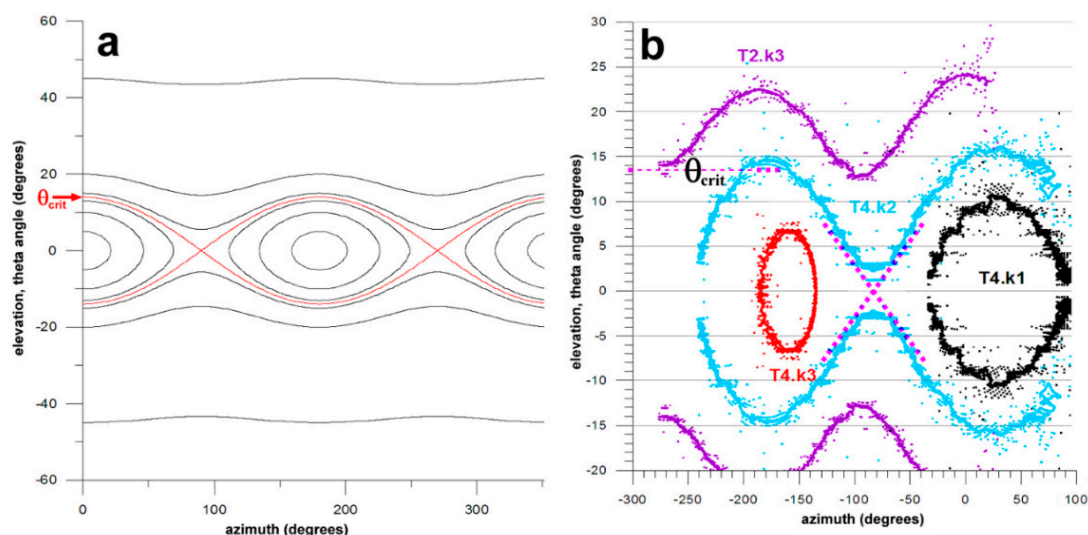


Figure 3. Elevation angle (pitch) of the ω -vector vs. azimuth angle (yaw) diagram (where the yaw angle is the position of the ω -vector in the ω_1 – ω_2 plane, and the pitch angle ω is the included angle between ω -vector and ω_1 – ω_2 plane); (a) polhode diagram for θ_{crit} of 13.5° (the red polhode indicates the separatrix condition); (b) experimental data on four kicks (the data were mirrored about $\theta = 0^\circ$); the crossed dashed lines indicate the separatrix condition; $\theta_{crit} \sim 13.5^\circ$.

5. Discussion

There are other ways of determining the MOI of an object about a specific axis, such as the pendulum method. The method used in this study, however, has the advantage that the behaviour of the ω -vector changes immediately when crossing the separatrix polhode.

It has to be borne in mind that the axes, about which an object spins and its ω -vector precesses, are not identical. In the ball shown in Figure 2c, the ω -vector precesses about the major axis while the ball spins about the minor axes with a slightly elevated and tilted ω -vector. The latter fact defines the kick as a drop punt. Thus, the critical angle θ_{crit} cannot be used for classification of, and distinction between, drop punts and torpedo punts.

That I_1 and I_2 turned out to be different, even only slightly, is an effect of the instrumentation as well as of the valve. The instrumentation was protected by an electronics box with a rectangular cross section such that $I_1 > I_2$. The valve alone (two semi-cylindrical pieces of rubber) had the same effect ($I_1 > I_2$). Nevertheless, even if that small difference in MOI can be ignored mechanically, it does make a difference in terms of the ω -vector's behaviour. The latter is characterized by changing the axis about which it precesses. These principles should be known to researchers and practitioners dealing with smart balls, in order to interpret the sensor data correctly.

Acknowledgments: No funds were received for conducting this study, nor for covering the costs to publish in open access.

Conflicts of Interest: The author declares no conflict of interest.

References

1. Ginsberg, J.H. *Engineering Dynamics*; Cambridge University Press: Cambridge, UK, 2008; Volume 10.
2. Fuss, F.K.; Smith, M.R. Development of a smart oval ball for assessment of angular flight dynamics and precision of kick execution. *Sports Tech.* **2011**, *4*, 151–158, doi:10.1080/19346182.2012.726224.
3. Fuss, F.K.; Smith, M.R.; Leali, F. Kick precision and spin rate in drop and torpedo punts. *Procedia Eng.* **2013**, *60*, 448–452, doi:10.1016/j.proeng.2013.07.011.



© 2020 by the authors. Licensee MDPI, Basel, Switzerland. This article is an open access article distributed under the terms and conditions of the Creative Commons Attribution (CC BY) license (<http://creativecommons.org/licenses/by/4.0/>).